Human Mesenchymal Stem Cells Overexpressing the IL-33 Antagonist Soluble IL-1 Receptor–Like–1 Attenuate Endotoxin-Induced Acute Lung Injury

Itziar Martínez-González[1], Oriol Roca[2,5], Joan R. Masclans[2,5], Rafael Moreno[1]*, Maria T. Salcedo[3], Veerle Baekelandt[6], Maria J. Cruz[4,5], Jordi Rello[2,5], and Josep M. Aran[1]

[1]Human Molecular Genetics Group, Institut d'Investigació Biomèdica de Bellvitge, L'Hospitalet de Llobregat, Barcelona, Spain; [2]Department of Critical Care, [3]Department of Pathology, and [4]Department of Pneumology, Vall d'Hebron University Hospital, Vall d'Hebron Research Institute, Universitat Autònoma de Barcelona, Barcelona, Spain; [5]Ciber Enfermedades Respiratorias, Instituto de Salud Carlos III, Madrid, Spain; and [6]Laboratory for Neurobiology and Gene Therapy, Department of Molecular Medicine, Katholieke Universiteit Leuven, Leuven, Belgium

Acute lung injury (ALI) and acute respiratory distress syndrome (ARDS) are characterized by pulmonary edema attributable to alveolar epithelial–interstitial–endothelial injury, associated with profound inflammation and respiratory dysfunction. The IL-33/IL-1 receptor–like–1 (ST2) axis plays a key role in the development of immune–inflammatory responses in the lung. Cell-based therapy has been recently proposed as an effective alternative for the treatment of ALI and ARDS. Here, we engineered human adipose tissue–derived mesenchymal stem cells (hASCs) overexpressing soluble IL-1 receptor–like–1 (sST2), a decoy receptor for IL-33, in order to enhance their immunoregulatory and anti-inflammatory properties when applied in a murine ALI model. We administered both hASCs and hASC-sST2 systemically at 6 hours after intranasal LPS instillation, when pathological changes had already occurred. Bioluminescence imaging, immunohistochemistry, and focused transcriptional profiling confirmed the increased presence of hASCs in the injured lungs and the activation of an immunoregulatory program (CXCR-4, tumor necrosis factor–stimulated gene 6 protein, and indoleamine 2,3-dioxygenase up-regulation) in these cells, 48 hours after endotoxin challenge. A comparative evaluation of hASCs and the actions of hASC-sST2 revealed that local sST2 overproduction by hASC-sST2 further prevented IL-33, Toll-like receptor–4, IL-1β, and IFN-γ induction, but increased IL-10 expression in the injured lungs. This synergy caused a substantial decrease in lung airspace inflammation and vascular leakage, characterized by significant reductions in protein content, differential neutrophil counts, and proinflammatory cytokine (TNF-α, IL-6, and macrophage inflammatory protein 2) concentrations in bronchoalveolar lavage fluid. In addition, hASC-sST2–treated ALI lungs showed preserved alveolar architecture, an absence of apoptosis, and minimal inflammatory cell infiltration. These results suggest that hASCs genetically engineered to produce sST2 could become a promising therapeutic strategy for ALI/ARDS management.

Keywords: inflammation; alveolar injury; cell therapy; IL-33

(*Received in original form October 9, 2012 and in final form April 25, 2013*)

* Rafael Moreno is now at the Translational Research Laboratory, Institut d'Investigació Biomèdica de Bellvitge-Institut Català d'Oncologia, L'Hospitalet de Llobregat, 08908 Barcelona, Spain.

This work was supported by the Federación Española de Fibrosis Quística and by Generalitat de Catalunya grant 2009SGR1490 (J.M.A.), by fellowships from the Associació Catalana de Fibrosi Quística (I.M.-G.), and by La Caixa and the Vall d'Hebron Research Institute (O.R.). J.M.A. is also sponsored by the Researchers Stabilization Program of the Sistema Nacional de Salud–Departament de Salut Generalitat de Catalunya (Exp. CES06/012).

Correspondence and requests for reprints should be addressed to Josep M. Aran, Ph.D., Human Molecular Genetics Group, Institut d'Investigació Biomèdica de Bellvitge, L'Hospitalet de Llobregat, Gran Vía s/n, km 2.7, 08908 Barcelona, Spain. E-mail: jaran@idibell.cat

This article has an online supplement, which is accessible from this issue's table of contents at www.atsjournals.org

Am J Respir Cell Mol Biol Vol 49, Iss. 4, pp 552–562, Oct 2013

Originally Published in Press as DOI: 10.1165/rcmb.2012-0406OC on May 8, 2013
Internet address: www.atsjournals.org

Acute lung injury (ALI) and its most severe form, the acute respiratory distress syndrome (ARDS), are leading causes of acute respiratory failure in critically ill patients, with a variety of disorders including sepsis, pneumonia, major trauma, acute pancreatitis, and drug overdose (1). The lung pathogenesis of ALI/ARDS is characterized by the sequestration of neutrophils, the up-regulation of proinflammatory mediators both systemically and locally, and disruption of the alveolar–capillary membrane barrier. This leads to the development of noncardiogenic proteinaceous alveolar edema and the subsequent impairment of lung mechanics within hours to days of a predisposing insult, such as bacterial infection. Despite advances in supportive treatment, mainly related to protective ventilation (2) and a fluid conservative strategy (3), the morbidity and mortality of patients remain unacceptably high (4). Therefore, innovative therapeutic strategies are actively being pursued to improve prognoses.

Evidence has shown that mesenchymal stem cells (MSCs) display not only low immunogenicity, but are also capable of modulating the activity of innate and adaptive immune cells such as dendritic cells, T cells, and B cells (5, 6), and are thereby anti-inflammatory. Furthermore, MSCs given intravenously temporarily localize in the lungs and thus provide a local source of trophic factors in the pulmonary environment (7, 8). Because the immune–inflammatory process seems to play a major role in both the alveolar epithelial and endothelial cell damage occurring in ALI/ARDS, recent studies have suggested a therapeutic benefit of MSC transplantation in different animal models of acute pulmonary inflammation/injury (9, 10).

Moreover, beyond the attractive intrinsic features of MSCs, they have a potential use as vectors or factories of desirable paracrine factors or other gene products through *ex vivo* genetic engineering, which may bring additional benefits in therapeutic cell transplantation for a number of diseases with limited treatment options, such as ALI/ARDS (11, 12).

IL-33 (interleukin-1 family member 11), the newest member of the IL-1 family of cytokines, has been recently characterized as a ligand for the orphan IL-1 receptor-like-1 (ST2) receptor, and it has been suggested to function as an alarmin because it is released upon endothelial or epithelial cell damage (13). The interaction of IL-33 with ST2 is involved in the early induction and further amplification of both the Th1 and Th2 immune–inflammatory responses, depending on the type of activated cell and the microenvironment of the damaged tissue (14). Two major products of the *ST2/T1* gene, a transmembrane form (ST2L) and a soluble form (sST2), are produced by alternative splicing under the control of two distinct promoters. ST2L is considered to be the functional component for the induction of IL-33 activities, whereas sST2 acts as a decoy receptor for IL-33. Furthermore, sST2 has been postulated as a repressor on its own of proinflammatory cytokine production by LPS-exposed macrophages, via the inhibition of Toll-like receptor–4 (TLR-4) expression (15).

In this study, we aimed to assess the anti-inflammatory and restorative capabilities of infusing sST2-overexpressing human adipose tissue–derived MSCs (hASC-sST2), to alleviate the pathological events occurring in a murine LPS-induced lung injury model. This combined gene and cell therapy strategy may prove particularly beneficial in the treatment of ALI/ARDS.

MATERIALS AND METHODS

hASC Isolation

Discarded human adipose tissue from two healthy adult women undergoing elective lipoaspiration was used as the source of hASCs throughout this study, under Institutional Ethics Committee approval, as described elsewhere (16). The isolated hASCs were expanded for 4 to 5 days (Passage 0), substituting the culture medium every 2 days until achieving 80% confluence, and were amplified through periodic passaging (split ratio, 1:2).

Lentiviral Vector Production and hASC Transduction

Transient triple-transfection on human embryonic kidney 293T cells, as previously described (16), produced vesicular stomatitis virus G protein–pseudotyped, high-titer lentiviral particles from pWPT-sST2FLAG2AEGFP (a bicistronic lentiviral vector encoding the sST2–C-terminal FLAG tag fusion and the enhanced green fluorescent protein (EGFP) cDNA sequences, separated by the porcine teschovirus-1 2A sequence) (17) and from its corresponding control counterpart pWPT-EGFP. The hASCs administered throughout the *in vivo* ALI model assays were transduced with the appropriate lentiviral vector particles at an optimized multiplicity of infection (MOI) of 20.

Murine Model of LPS-Induced ALI and Study Design

Ten- to 12-week-old male BALB/c mice (Harlan, Horst, The Netherlands) were anesthetized with 2% isoflurane and challenged with a single intranasal instillation of 8 mg/kg LPS (*Escherichia coli* 055:B5; Sigma-Aldrich, St. Louis, MO), dissolved in 50 μl of PBS, or else the mice received 50 μl of PBS alone. Six hours after the induction of injury, mice received engineered hASCs expressing the reporter EGFP (hASCs), engineered hASCs expressing the sST2-2A–EGFP fusion (hASC-sST2; 1×10^6 cells in 200 μl of PBS in both cases), or 200 μl of PBS by tail-vein injection. All mice were analyzed at 48 hours after LPS/PBS instillation. For each batch of hASC-sST2 used, we confirmed adequate sST2 protein expression levels by ELISA, as previously indicated.

All procedures involving mice were reviewed and approved by the Ethics Committee of Animal Experimentation at the Vall d'Hebron Research Institute (Barcelona, Spain; CEEA study number 61/09).

Bronchoalveolar Lavage, Cell Count, and Protein Measurement

Bronchoalveolar lavage (BAL) was performed in the treated mice at 48 hours after intranasal instillation. The lungs were lavaged three times *in situ* with 0.7 ml of sterile saline (0.9% NaCl) at room temperature, and the recovered fluid was pooled. Cells were counted with a hemocytometer (total cells), and the BAL fluid (BALF) was centrifuged ($1{,}500 \times g$, 10 min). The supernatant was frozen (-80°C) until further analysis. Total protein was measured in the BALF with the bicinchoninic acid assay (Pierce, Rockford, IL).

BALF and Plasma Cytokine/Chemokine Assessment

We measured concentrations of murine TNF-α, IL-6 (both from Diaclone, Besançon Cedex, France), macrophage inflammatory protein 2 (MIP-2; IBL, Gunma, Japan), and IL-33 (R&D Systems, Abingdon, UK) in undiluted BALF and in serum (from blood drawn via cardiac puncture, and centrifuged for 30 min at $2{,}000 \times g$) by ELISA, according to the manufacturer's instructions.

Histopathology and Immunohistochemistry

Tracheas from hASC-treated, hASC-sST2–treated, and PBS-treated ALI animals not undergoing BAL were cannulated at 48 hours after LPS/PBS intranasal instillation, and the lungs were fixed by inflation to total lung capacity with 1 ml of 4% paraformaldehyde under a constant inflation pressure of 25 cm H_2O. After overnight fixation, lung tissue was embedded in paraffin, cut into 3-μm-thick sections, and stained with hematoxylin and eosin.

For immunohistochemistry, formalin-fixed tissues were dehydrated with an ethanol gradient, cut, and embedded in paraffin. Sliced 5-μm sections were mounted on poly-L-lysine–coated glass slides and immunostained as previously described (18).

Detailed methodologies for the isolation and characterization of hASCs, sST2 cloning, hASC transduction, Western blot analysis, IL-33–sST2 interactions, bioluminescence imaging, RNA isolation and analysis, differential cell counts, the flow cytometry of BALF cells, histopathology, immunohistochemistry, and the measurement of lung mechanics are described in the online supplement.

Statistical Analysis

Unless indicated otherwise, we represent data as mean values ± SEMs, or as individual points in a vertical dot plot, with a line to indicate the mean value. We used one-way ANOVA, adjusted for multiple comparisons (Bonferroni test), or an unpaired *t* test for statistical analyses (GraphPad Prism, version 5.00; GraphPad Software, Inc., San Diego, CA). In all instances, we considered $P < 0.05$ statistically significant.

RESULTS

Behavior of Transplanted hASCs in the Mouse ALI Model: Biodistribution and Activation

A thorough phenotypic and functional characterization was first performed on the adherent fibroblast-like hASCs isolated from lipoaspirates (16) (Figure E1 in the online supplement). The lentiviral vector-mediated transduction of hASCs with the bicistronic EGFP-2A–firefly luciferase configuration (19) (Figure 1A) facilitated the sensitive tracking of the infused hASCs by bioluminescence imaging. Therefore, we confirmed the retention and further gradual clearance of intravenously infused hASCs in the lungs of healthy mice, lasting nearly 1 week (Figure E2). Moreover, flow cytometric analysis of the EGFP-positive cells stained with the macrophage-1 antigen (MAC-1) from the BALF of ALI mice, generated by intranasal instillation of the endotoxin LPS, indicated that phagocytosis by mouse alveolar macrophages might contribute, at least in part, to hASC clearance (Figure E3). Next, we evaluated the *in vivo* organ biodistribution of hASCs at two different times after their intravenous administration in the mouse ALI model, as already described. The exclusive presence of the bioluminescent signal in the lungs of transplanted animals, irrespective of PBS or LPS instillation, confirmed the retention of intravenously infused hASCs throughout the pulmonary parenchyma (Figures 1B and 1C). Interestingly, at 48 hours after transplantation, a significantly increased presence of hASCs was evident in the LPS-instilled lungs compared with the PBS-instilled control lungs (Figures 1B–1D). This increase was probably attributable to transient hASC expansion in the injured environment, because the transcript levels of the human Ki67 proliferation marker from both LPS-instilled and PBS-instilled mice were found to be the same at 48 hours after hASC infusion (Figure 2A). Indeed, an analogous outcome was observed *in vitro*, after hASC induction with different proinflammatory stimuli (Figure E4).

On the other hand, hASC activation in the LPS-induced proinflammatory milieu of the lung was evident because of significant up-regulation of the chemokine receptor CXCR-4, which is critical for the trafficking of MSCs toward the stromal cell–derived factor–1α secreted at injury sites (20), and of key anti-inflammatory and immunosuppressive transcripts encoding soluble factors such as the IL-1/TNF-inducible protein tumor necrosis factor–stimulated gene 6 protein (TSG-6); the indoleamine 2,3-dioxygenase (IDO)

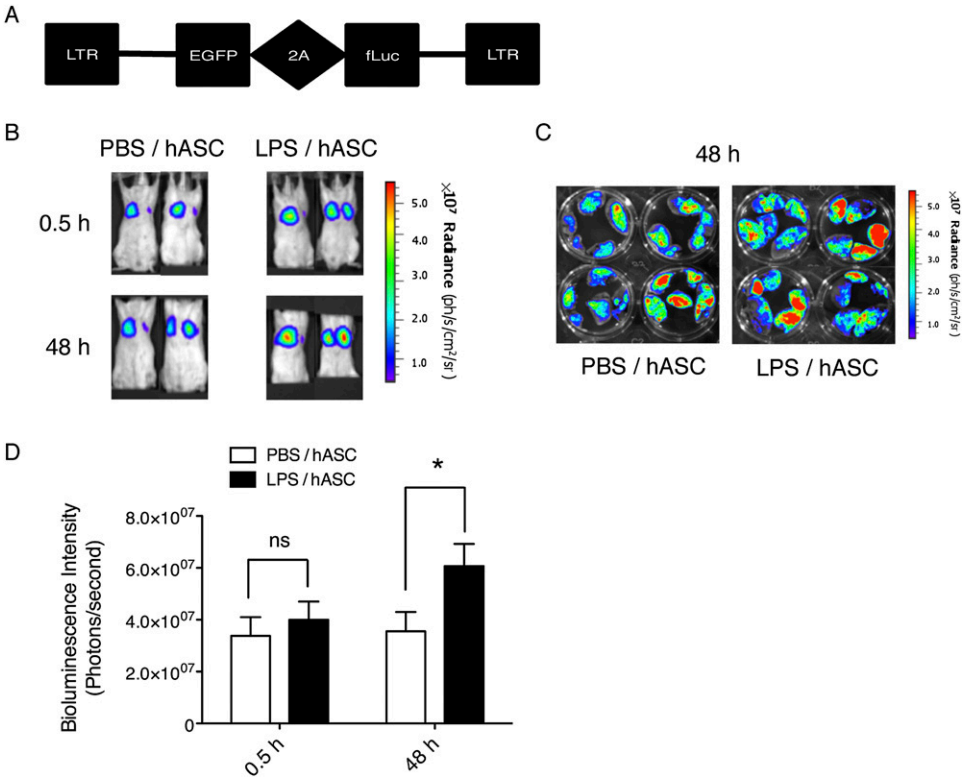

Figure 1. Noninvasive *in vivo* imaging of human adipose tissue–derived mesenchymal stem cell (hASC) biodistribution into unchallenged and endotoxin-challenged mice with acute lung injury (ALI). (*A*) Schematic proviral configuration of the lentiviral vector with peptide 2A sequence (LV-T2A) lentiviral vector used. The resulting bicistronic transcript contains, in a 5′ to 3′ orientation, the enhanced green fluorescent protein (EGFP) reporter gene, followed by the picornavirus-derived 2A peptide mediating cotranslational cleavage from the second cistron, the firefly luciferase (fLuc) gene. (*B*) Bioluminescent signals as a consequence of fLuc activity generated by LV-T2A–transduced hASCs intravenously injected into mice (1×10^6 cells/mouse). Graphic images were recorded at 0.5 hour and 48 hours after hASC administration in both control PBS-instilled mice (*left*) and LPS-instilled mice (*right*), with a 6-hour interval between instillation and cell administration (two representative animals per group are shown). The *color scale* (represented in photons/s/cm^2/steradian) next to the images indicates signal intensity, where *red* and *blue* represent the highest and lowest signal intensities, respectively. (*C*) Graphic images show the *ex vivo* bioluminescent signal detected in excised lung lobes from four representative animals per group at 48 hours after intravenous LV-T2A–transduced hASC administration. (*D*) Bar diagram of *in vivo* fLuc activity quantification. Photon flux (ph/s) values were extracted from the recorded images (*above*) and plotted versus the elapsed time after hASC inoculation, after background subtraction ($n = 10$ mice per group). *$P < 0.05$, LPS compared with PBS. ns, not significant.

enzyme, involved in tryptophan catabolism; and, to a lesser extent, the inducible prostaglandin-producing enzyme cyclooxygenase-2 (COX-2) and the immunoregulatory cytokine transforming growth factor (TGF)–β (Figure 2A). All these mediators play a central role in the immunomodulatory actions of MSCs (6, 21).

Furthermore, immunostaining of human Ki67 protein from infused, mitotically active hASCs revealed appreciable differences in their cellular localization. Thus, in the lung tissue from PBS-instilled mice, hASCs were sparsely present, and were distributed as discrete small clusters likely retained within the alveolar microcapillaries. In contrast, in LPS-induced mice, hASCs showed a more abundant and scattered presence throughout the lung parenchyma (Figure 2B).

Thus, the acute proinflammatory lung-injury environment seems to induce an anti-inflammatory and immunomodulatory activation program in lung-retained hASCs.

Generation and Characterization of hASCs Overexpressing Murine sST2

Growing evidence supports an important role for IL-33 in innate airway inflammation. Thus, we explored whether the genetic engineering of hASCs as vectors and factories of the IL-33 decoy receptor sST2 could endow them with additional or synergistic therapeutic benefits when transplanted into an ALI mouse model.

Therefore, we designed a bicistronic lentiviral vector incorporating a picornaviral 2A sequence flanking at a 5′ to 3′ orientation the C-terminus FLAG-tagged murine sST2 cDNA and the reporter EGFP cDNA (Figure 3A). The transduction of hASCs with the lentiviral vector confirmed the cotranslational cleavage of the polyprotein product into the murine sST2-FLAG peptide and the reporter EGFP, according to Western blot analysis. The EGFP reporter also permitted us to visualize and estimate the transduction efficiency of hASCs by both flow cytometry and fluorescence microscopy (Figure 3B). In addition, increasing the MOI was correlated with an augmented production and secretion of recombinant murine sST2 by hASCs. Thus, at a MOI of 20, we reached an average 80% ± 5% transduction efficiency, and a concentration of secreted sST2 (35 ± 15 ng/ml) comparable to that induced by the LPS treatment of National Institutes of Health 3T3 fibroblasts (Figure 3C). This optimized MOI of 20 was selected for the transduction of hASCs used in all *in vivo* administration assays. Furthermore, we evaluated the functionality of the recombinant murine sST2-FLAG secreted by the transduced hASCs. The sST2-FLAG decoy was able to interfere significantly, in a dose-dependent manner, with IL-33–T1/ST2 signaling in P815 mouse mastocytoma cells by reducing the induction of proinflammatory IL-6 (22) (Figure 3D). As previously reported (16), lentiviral vector-mediated hASC transduction did not change their phenotype and functional properties (data not shown).

Superior Therapeutic Effects of hASCs Overexpressing sST2 on Acute LPS-Induced Pulmonary Inflammation

The IL-33–ST2 axis plays a key role in bridging innate and adaptive immune responses in the lung during infection, inflammation, and tissue damage (13). Therefore, we sought to elucidate whether combining sST2-mediated local IL-33 blockade and the inherent anti-inflammatory and immunomodulatory actions of hASCs yielded a therapeutic effect superior to that of administering hASCs alone in a murine model of ongoing ALI induced by LPS (Figure 4A). LPS triggers a large influx of polymorphonuclear cells into the airspaces. This influx peaks at around 48 hours, and is associated with increased microvascular permeability (23).

Macroscopically, LPS-instilled and PBS-treated mice evidenced overt symptoms of endotoxemia at 48 hours after challenge,

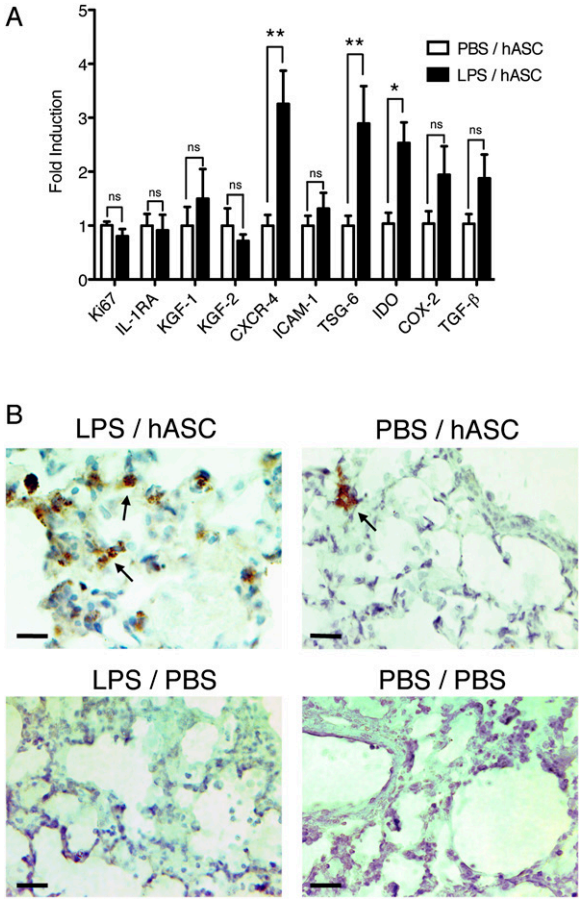

Figure 2. Activation status of hASCs after intrapulmonary retention in the mouse ALI model. (*A*) The relative mRNA expression of the proliferation marker gene human Ki67 and of the hASC activation–related genes IL-1RA, keratinocyte growth factor (KGF)-1, KGF-2, CXCR-4, intercellular adhesion molecule–1 (ICAM-1), tumor necrosis factor–stimulated gene 6 protein (TSG-6), indoleamine 2,3-dioxygenase (IDO), cyclooxygenase-2 (COX-2), and transforming growth factor (TGF)–β in hASC-treated murine lung tissue was determined by TaqMan quantitative RT-PCR with the corresponding human-specific probes, and normalized through the housekeeping gene GUSB. Data are presented as fold induction of the indicated gene from LPS-challenged and hASC-treated mice (LPS/hASC; *solid bars*), relative to the same gene from PBS-instilled and hASC-treated mice (PBS/hASC; *open bars*) ($n = 3$–6). $^*P < 0.05$. $^{**}P < 0.01$. ns, not significant. (*B*) Representative immunohistochemical images of human Ki67-stained lung tissue from hASC-treated mice at 48 hours after LPS induction (LPS/hASC) or PBS instillation (PBS/hASC) (*above*). Corresponding control images of Ki67-stained lung tissue from LPS-instilled and PBS-instilled and untreated mice (*below*). *Arrows* indicate positive staining. *Scale bar* = 20 μm.

characterized by a hunched appearance, raised hair, sweating, reduced locomotor and exploratory behavior, and decreased responses to external stimuli. In contrast, mice instilled with LPS and treated with hASCs or hASC-sST2 at 6 hours after endotoxin challenge showed a lesser degree of sickness when evaluated for the same symptoms. Moreover, a preliminary gross lung examination of the LPS-injured mice revealed that the PBS-treated animals contained petechial hemorrhages and necrotic lung lobes. By contrast, considerably fewer morphological alterations or lesions were seen in the lungs from LPS-instilled plus hASC-treated and, particularly, from LPS-instilled plus hASC-sST2–treated mice (Figure 4B).

hASCs overexpressing the sST2-FLAG transgene were immunolocalized in the LPS-injured lungs from all hASC-sST2–transplanted mice, which evidenced the local delivery of this anti-inflammatory decoy into the inflamed lung parenchyma (Figure 4C, *left column*). Furthermore, the presence of hASCs in the transplanted lungs was confirmed by reporter EGFP expression (Figure 4C, *right column*).

It was suggested that endotoxin-induced ALI could be regulated by both the ST2–IL-33 and the ST2–TLR4 axes (15, 24). Therefore, we assessed whether hASCs on their own, or hASCs overexpressing transgenic sST2, would be able to modulate the expression of the ST2-related proinflammatory mediators IL-33 and TLR4, as well as other relevant inflammatory cytokines such as IL-1β, IFN-γ, and IL-10 in LPS-injured lungs. Indeed, whereas hASC treatment was able to reduce the expression of the proinflammatory mediators IL-33, TLR4, IL-1β, and IFN-γ to different degrees in LPS-challenged mice, hASC-sST2 treatment not only fully prevented their transcriptional induction, but also significantly up-regulated the anti-inflammatory cytokine IL-10, as determined by the quantitative RT-PCR of mRNA isolated from lung homogenates (Figures 5A and 5B).

In addition, although undetectable in the BALF, increased proinflammatory IL-33 production was observed in the sera of LPS-instilled mice at 48 hours after challenge. Interestingly, treating mice with hASC-sST2 precluded the LPS-mediated overproduction of circulating IL-33 (Figure 5C).

Notably, when compared with PBS-instilled control mice, LPS-instilled mice experienced marked proinflammatory alterations in the lungs, such as pulmonary vascular leakage, edema, and immune cell shedding into the epithelial lining fluid at 48 hours after endotoxin challenge. Conversely, immune cell counts (Figure 6A), neutrophil counts (Figure 6B), and total protein content (Figure 6C) in the BALF of hASC-treated mice were decreased with respect to those observed in untreated mice. Remarkably, both the proinflammatory cellular infiltrates and the lung vascular barrier compromise observed in endotoxin-treated mice were further attenuated by sST2 overexpression in hASC-sST2–treated lungs.

Increased amounts of both the proinflammatory cytokines TNF-α and IL-6, and the neutrophil chemoattractant MIP-2, are known to be actively involved in the pathophysiology of endotoxin-mediated pulmonary inflammation. Notably, the concentrations of TNF-α, IL-6, and MIP-2 were found to be significantly reduced in the BALF of LPS-challenged and hASC-sST2–treated mice, compared with those concentrations in LPS-challenged and untreated mice (Figures 6D–6F). However, hASC treatment after LPS challenge yielded intermediate BALF cytokine/chemokine concentrations. The same trend was also perceived in the sera of the analyzed animals, although the concentrations of these proinflammatory mediators were at just about the threshold of detection (data not shown).

Moreover, a blinded histopathological examination of lung sections from the LPS-induced, untreated mice revealed a marked inflammatory infiltrate consisting of polymorphonuclear leukocytes and macrophages at 48 hours after endotoxin challenge, which was slightly reduced in LPS-induced and hASC-treated mice. In addition, hASC-sST2 treatment further reduced the immune–inflammatory infiltrates present in LPS-challenged mice, leading to an improved histological appearance similar to that from unchallenged control mice (i.e., preserved lung architecture and better tissue-injury scoring) (25) (Figures 7A and 7C). Likewise, hASC treatment prevented the widespread apoptosis and necrosis of bronchial tissue (i.e., epithelial cells and infiltrating neutrophils) induced after LPS instillation, as assessed by terminal deoxynucleotidyl transferase–mediated deoxyuridine triphosphate nick-end labeling staining (Figure 7B).

Finally, although our lung injury model was mainly designed to evaluate reversions of acute lung inflammation, we also explored the quantification of mechanical parameters from a pulmonary functional standpoint through forced oscillation mechanics.

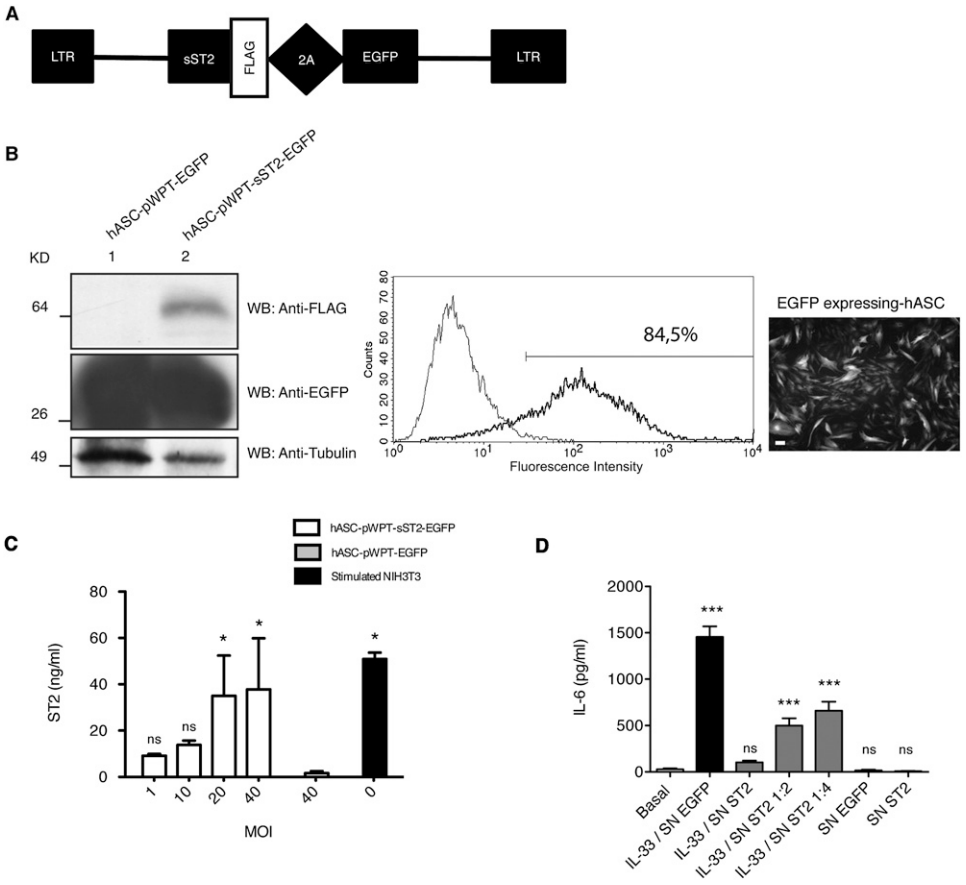

Figure 3. Generation and characterization of genetically engineered hASCs overexpressing soluble IL-1 receptor–like–1 (sST2). (*A*) Schematic proviral configuration of the pWPT-sST2FLAG2AEGFP (pWPT-sST2-EGFP) lentiviral vector used. The resulting bicistronic transcript contains, in a 5′ to 3′ orientation, sequences encoding the C-terminus FLAG-tagged murine sST2 gene, followed by the picornavirus-derived 2A peptide mediating cotranslational cleavage from the second cistron, the EGFP reporter gene. (*B*) *Left*: pWPT-sST2-EGFP–transduced hASCs express both the sST2 and the EGFP transgenes. sST2 and EGFP protein expression was assessed in cell extracts by Western blotting. *Top blot*: Detection of the specific 64-kD sST2-FLAG band in hASCs transduced with pWPT-sST2-EGFP (*lane 2*), but not in hASCs transduced with the control counterpart pWPT-EGFP (*lane 1*), both at multiplicity of infection (MOI) = 20. *Middle blot*: The reporter EGFP protein was detected in both pWPT-sST2-EGFP–transduced and pWPT-EGFP–transduced hASCs. *Bottom blot*: Endogenous tubulin expression. *Center*: Representative flow cytometric histogram overlay of pWPT-sST2-EGFP–transduced hASCs (MOI = 20) shows transduction efficiency as the percentage of EGFP-positive hASC (*dark line*) over the autofluorescent background from nontransduced hASCs (*gray line*). *Right*: EGFP expression of pWPT-sST2-EGFP–transduced hASCs (MOI = 20) by fluorescence microscopy. *Scale bar* = 200 μm. (*C*) sST2 protein expression was assessed in cell-culture supernatants by ELISA. The concentrations of murine sST2 were evaluated from supernatants collected 48 hours after lentiviral transduction at the indicated MOIs. *Open columns*, pWPT-sST2-EGFP–transduced hASCs. *Gray column*, pWPT-EGFP–transduced hASCs. The sST2 concentrations of National Institutes of Health 3T3 mouse fibroblast supernatants induced with LPS (10 μg/ml) for 48 hours were determined for comparison (*solid column*). Data are presented as means ± SDs ($n = 3$). *$P < 0.05$, compared with pWPT-EGFP–transduced hASC supernatants. ns, not significant. (*D*) sST2-FLAG secreted from pWPT-sST2-EGFP–transduced hASCs interferes with IL-33–T1/ST2 (IL-1 receptor-like-1)–mediated IL-6 production by P815 mastocytoma cells. Before stimulation, IL-33 (1 ng/ml) was coincubated for 15 minutes at 37°C with culture supernatants from pWPT-EGFP–transduced hASCs (SN-EGFP), or from pWPT-sST2-EGFP–transduced hASCs (SN-sST2), at different dilutions (undiluted, 1:2, and 1:4). The resultant mixtures were added to P815 cells for 48 hours, and the induced IL-6 concentrations were assessed in the corresponding culture supernatants by ELISA. Control samples included untreated P815 supernatants (basal), and noninduced (no IL-33), SN-EGFP–treated, or SN-sST2–treated supernatants. Results shown are presented as means ± SDs, including triplicate measurements from three independent experiments. ***$P < 0.001$, compared with the basal, noninduced P815 cell supernatant. ns, not significant; WB, Western blot.

Therefore, at 48 hours after endotoxin challenge, tissue damping or energy dissipation and lung-tissue elastance tended to increase in LPS-induced mice compared with PBS-instilled control mice. In contrast, both mechanical parameters were reduced to control values in both hASC-treated and hASC-sST2–treated mice after LPS induction (Figure E5).

DISCUSSION

In this study, we have approached a combined strategy of gene-based and cell-based therapy to comprehensively modulate the ongoing pulmonary immune–inflammatory process induced by intranasal LPS instillation in an endotoxin-based murine ALI model. For that purpose, we first isolated and characterized hASCs (16), and further exploited their immunomodulatory and anti-inflammatory properties (5, 6, 21) in endotoxin-injured lungs.

An additional attractive feature of MSCs relates to their lung retention after systemic administration. The intravenous infusion of MSCs has been shown to lead to their homogeneous distribution into the lung parenchyma (7, 26), attributable to a known cell-trapping phenomenon occurring in the pulmonary microvasculature (27). Moreover, through *in vivo* bioluminescence imaging, we demonstrated that LPS-induced injury significantly increased the presence of hASCs in the damaged lungs as a consequence of hASC recruitment (through CXCR-4 up-regulation) and activation. Indeed, we demonstrated the induction of an anti-inflammatory/immunosuppressive program in hASCs (TSG-6, IDO, and to a lesser extent, COX-2 and TGF-β overexpression) within stressed airways. Moreover, the pattern of mitotically active hASC distribution, as assessed by immunohistochemistry, changed from scarce and clustered in uninjured lungs, to spread out and more abundant in LPS-injured lungs, likely attributable to both the transient expansion and vascular leakage of activated hASCs (23), although additional studies will be needed to establish these points. Accordingly, recent reports have also shown both a significantly increased presence of MSCs in the lungs of a ragweed-induced allergic inflammation model when compared with the unchallenged state (28), and the activation or licensing of MSCs toward an anti-inflammatory, immunomodulatory state in different ALI models (9, 10).

In addition, we confirmed by bioluminescence analysis a gradual decay of the infused hASCs within the lungs of uninjured,

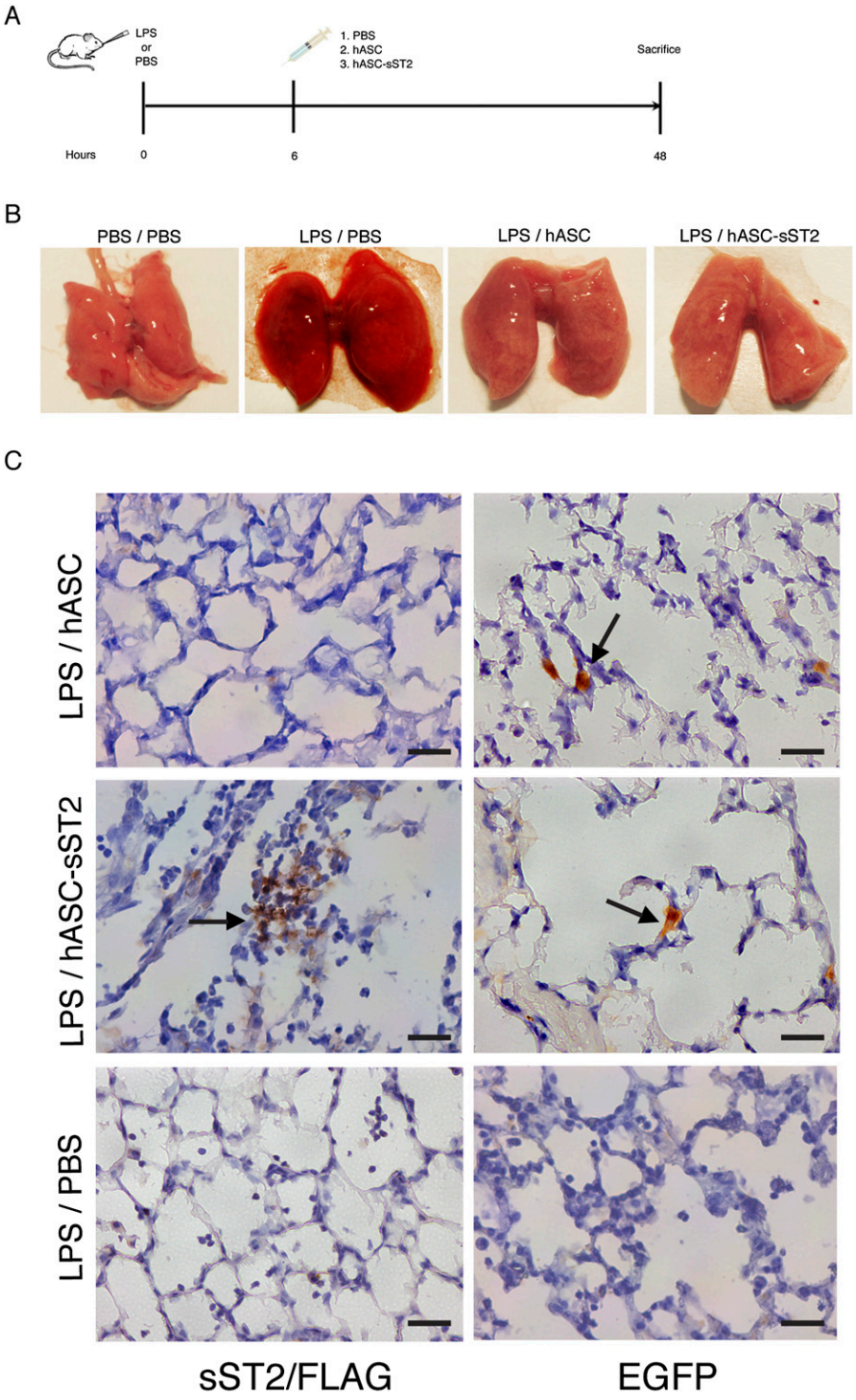

Figure 4. Engineered hASC transplantation in the endotoxin-induced ALI model. (*A*) Experimental design for the *in vivo* hASC transplantation study. BALB/c mice initially received LPS or PBS by nasal instillation, followed by intravenous injection 6 hours later of PBS, genetically engineered hASC-overexpressing EGFP (hASC), or genetically engineered hASCs overexpressing both sST2 and EGFP (hASC-sST2). Mice were killed 48 hours after the initial pathogenic challenge, to evaluate therapeutic efficacy. (*B*) Gross appearance of representative lungs from control, PBS-instilled mice (PBS/PBS); LPS-challenged, untreated mice (LPS/PBS); LPS-challenged plus hASC-treated mice (LPS/hASC); and LPS-challenged plus hASC-sST2–treated mice (LPS/hASC-sST2) at 48 hours after LPS instillation. (*C*) Immunohistochemical localization of genetically engineered hASCs overexpressing both murine sST2-FLAG and EGFP in endotoxin-injured lungs. Representative lung section images of LPS/hASC mice (*top*), LPS/hASC-sST2 mice (*middle*), and LPS/PBS control mice (*below*) at 48 hours after LPS instillation. *Arrows* indicate the *brown label* detection of sST2-FLAG–stained hASCs (*left column*), and of EGFP-stained hASCs (*right column*). *Scale bar* = 10 μm.

immunocompetent host mice. An analogous study in nude mice also reported lung retention and a further 1 week removal of intravenously infused hASCs, which suggests a predominant role of the innate immune system in hASC lung clearance (29). Indeed, flow cytometric analyses of EGFP and phycoerythrin–MAC-1 double-stained cells in the BALF from LPS-injured and hASC-treated mice suggest the contribution of alveolar macrophages as a relevant factor for hASC clearance in LPS-injured lungs. MSC-educated macrophages were recently reported to display anti-inflammatory and increased phagocytic activities (30). In contrast, hASCs seem to display a low susceptibility to natural killer (NK) cell–mediated lysis, which could be mediated through the actions of soluble factors such as IDO metabolites (31). Further studies will be needed to establish the relative contributions of the different innate and adaptive immune cells influencing hASC lung clearance. Nonetheless, because of the temporary pathological scenery of ALI/ARDS, our results suggest that in an adoptive cell-therapy strategy based on the transfer of allogeneic hASCs as "universal donors," the transferred cells would remain in the lung tissue long enough to balance the immune–inflammatory response before being cleared.

Several recent reports indicate the usefulness of human MSC administration in LPS-induced or *E. coli*–induced murine ALI. Three of these reports involved umbilical cord blood–derived

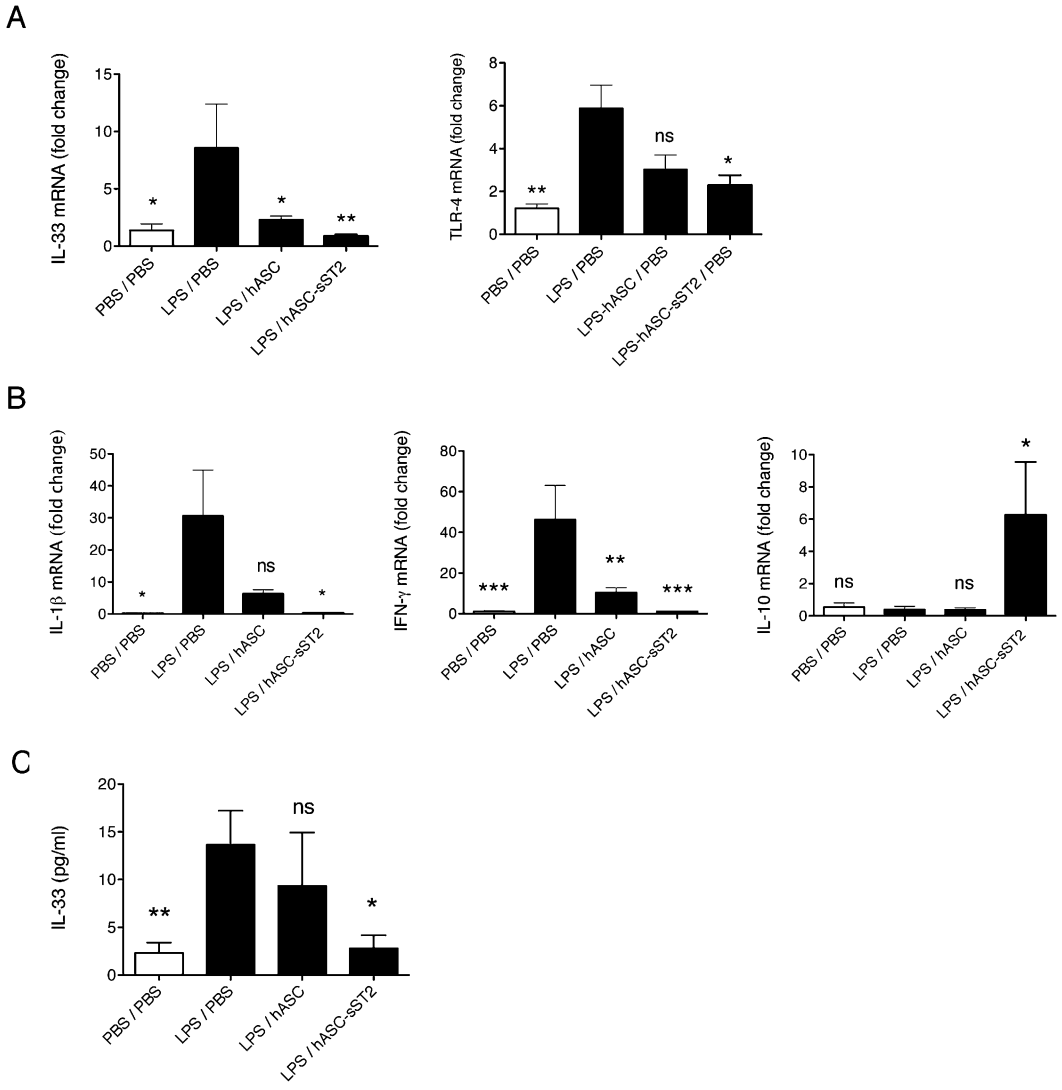

Figure 5. Involvement of proinflammatory IL-33/ST2/Toll-like receptor–4 (TLR4) signaling in the endotoxin-induced ALI model. (*A*) The relative mRNA expression of the murine transcripts IL-33 (n = 3–5 per group), TLR4 (n = 6–8 per group), IL-1β, IFN-γ, and IL-10 (n = 4–5 per group/each) were measured in lung tissue by TaqMan quantitative RT-PCR at 48 hours after LPS or PBS instillation, using the constitutively expressed Cebpa gene for normalization. Data are presented as fold induction of the indicated gene from LPS-challenged and untreated mice (LPS/PBS) or hASC-treated mice (LPS/hASC and LPS/hASC-sST2) (*solid columns*), relative to the same gene from PBS-instilled, untreated mice (PBS/PBS) (*open columns*). (*B*) Serum IL-33 concentrations from control, PBS-instilled (PBS/PBS) (*open column*), and LPS-challenged, untreated mice (LPS/PBS), LPS-challenged plus hASC-treated mice (LPS/hASC), and LPS-challenged plus hASC-sST2–treated mice (LPS/hASC-sST2) (*solid columns*) (n = 8–9 per group), were determined by ELISA, as indicated in Materials and Methods. *P < 0.05, **P < 0.01, and ***P < 0.001, compared with the LPS/PBS group. ns, not significant.

human MSCs, which reduced pulmonary inflammation and oxidative stress, enhancing alveolar $CD4^+CD25^+Foxp3^+$ T-regulatory cells and bacterial clearance (32–34). A comparative study of human and mouse ASCs also concluded that treatment with both cell sources was able to attenuate LPS-induced ALI significantly in mice (35). Nevertheless, none of these studies has characterized the biodistribution and/or activation state of infused human MSCs in the injured host. Furthermore, an interesting study assessing the activation status of bone marrow–derived human MSCs in LPS-induced ALI mice concluded that secreted TSG-6, which we also found to be up-regulated significantly, plays an essential anti-inflammatory role and contributes to reducing proinflammatory cytokines, neutrophil counts, and total protein in BALF (36). In all these studies, cell therapy was administered shortly after LPS challenge (30 min to 4 h). Thus, our results improve the therapeutic window of sST2-overexpressing hASC therapy by up to 6 hours after the intervention, when the inflammatory pathology has significantly progressed (34). Of note, Lee and colleagues (37, 38) have also shown that treatment with allogeneic human MSCs restored alveolar fluid clearance and reduced inflammation in *ex vivo* perfused human lungs injured by either *E. coli* endotoxin or live bacteria.

In addition, we sought to improve the therapeutic potential of hASCs in our ongoing ALI model through the overexpression of sST2, a decoy receptor for IL-33, by genetic engineering (hASC-sST2). We were particularly interested in targeting the proinflammatory cytokine IL-33 because it has been shown to interact with the T1/ST2 receptor and to induce not only Th2-type but also Th1-type immune responses (24, 39). At the transcriptional level, behind the immunomodulatory activity of unmodified hASCs, hASC-sST2 treatment was able to abrogate the expression of key proinflammatory mediators such as IL-33 itself, IL-1β, and IFN-γ that were significantly up-regulated in the lungs of our LPS-instilled ALI mice, and hASC-sST2 treatment concomitantly induced the anti-inflammatory cytokine IL-10. Accordingly, we found an increased production of IL-33 in the sera of LPS-instilled mice, which was attenuated to basal concentrations only after hASC-sST2 treatment, but not after hASC treatment. This finding is in agreement with IL-33 functioning in ALI as a "damage-associated molecular pattern" or alarmin, which is released on endothelial and epithelial cell damage, targeting resident innate immune cells, particularly in the lung alveoli (40). Recent reports have suggested a key role for IL-33 as an amplifier of innate immunity, and have shown that $IL\text{-}33^{-/-}$ mice were resistant to endotoxin shock in comparison with $IL\text{-}33^{+/+}$ mice after LPS injection (41). Furthermore, the ST2–IL-33 axis has been shown to increase the expression of the LPS receptor components lymphocyte antigen 96 (MD2) and TLR4 in macrophages, preferentially inducing the MyD88-dependent pathway, and this axis can also activate NK and invariant natural killer T

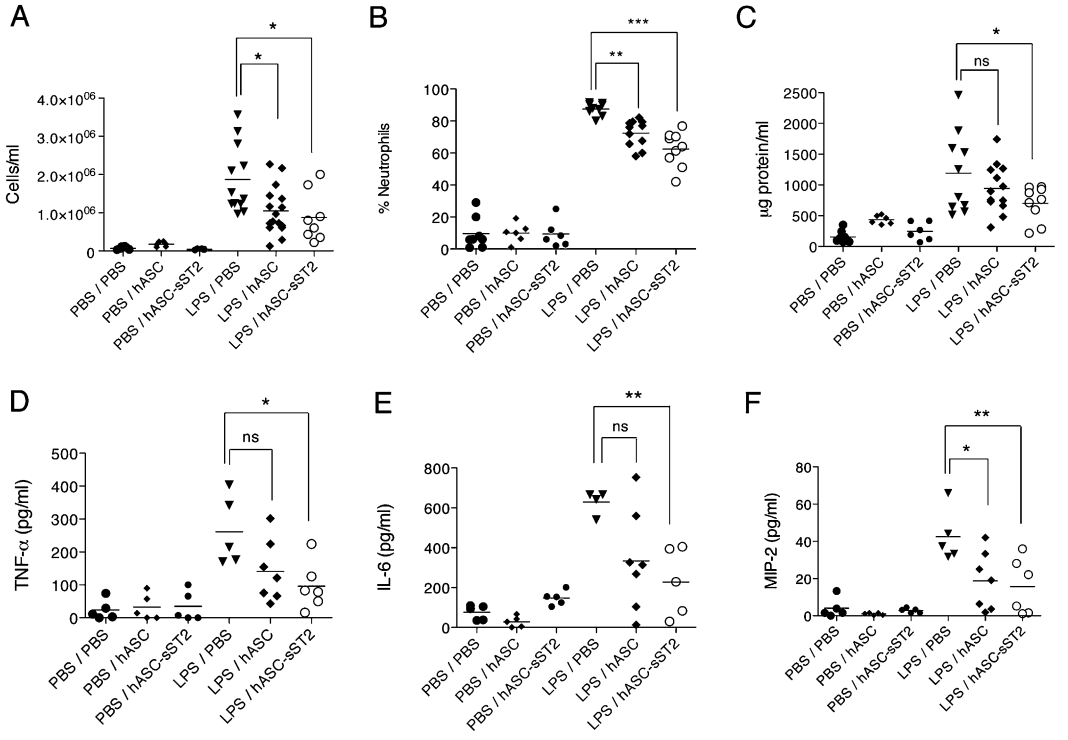

Figure 6. Bronchoalveolar lavage fluid (BALF) analyses after LPS-induced lung inflammation in mice. Numbers of inflammatory cells (*A*) and neutrophils (*B*) in the lung airspace, and vascular leakage measured by total protein accumulation in the BALF (*C*), were determined at 48 hours after LPS or PBS instillation (PBS-instilled groups, $n = 6–8$; LPS-challenged groups, $n = 8–16$). Concentrations of the proinflammatory cytokines TNF-α (*D*) and IL-6 (*E*), and of the chemokine macrophage inflammatory protein 2 (MIP-2) (*F*), were measured at 48 hours after LPS or PBS instillation through specific ELISAs ($n = 5–7$ per group). PBS/PBS, PBS-instilled, untreated mice; PBS/hASC, PBS-instilled, hASC-treated mice; LPS/PBS, LPS-challenged, untreated mice; LPS/hASC, LPS-challenged, hASC-treated mice; LPS/hASC-sST2, LPS-challenged, hASC-sST2–treated mice. $^*P < 0.05$, $^{**}P < 0.01$, and $^{***}P < 0.001$, compared with the LPS/PBS group. ns, not significant.

cells to produce Th1 cytokines (39). Thus, the local release of the sST2 decoy receptor by our engineered hASCs in endotoxin-injured lungs could complete a dual role, by (*1*) trapping IL-33 and preventing it from binding to T1/ST2 on the surface of various target cells, and (*2*) binding directly to macrophages through an undefined receptor and down-modulating TLR4 and TLR1 (15). Certainly, we have found a significant down-regulation of TLR4 in the lungs of ALI mice treated with hASC-sST2, compared with mice either untreated or hASC-treated.

Regarding the functional parameters dysregulated in ALI, our study demonstrates that hASC-sST2 treatment was superior to treatment with hASCs administered alone. Interestingly, hASC-sST2 treatment reduced pulmonary vascular leakage, leukocyte influx, and especially, neutrophil influx and proinflammatory TNF-α, IL-6, and MIP-2 in the BALF of LPS-challenged mice. This outcome was correlated with a minor degree of symptomatic sickness, and with a viable lung appearance both macroscopically (minimal petechial hemorrhages and an absence of necrotic lung lobes), and microscopically (preserved alveolar architecture and minimal inflammatory-cell infiltration). Furthermore, in LPS-injured lungs, both hASC and hASC-sST2 treatments were able to prevent extensive apoptosis/necrosis (42) and a short-term deterioration in respiratory function. Nevertheless, our pulmonary function analysis has been optimized for chronic murine models (43), and seems to have limited sensitivity in ALI models.

The adenovirus-mediated overexpression of sST2 was recently reported to provide a protective effect in mice with LPS-induced ALI (44), although in that study, gene transfer was performed before lung injury, which questions the effectiveness of a post-treatment strategy and its relevance for clinical therapy.

Furthermore, two studies pioneered the use of genetically engineered allogeneic MSCs overexpressing the vasculoprotective factor angiopoietin-1 (Ang-1) in the LPS-induced ALI model, and found that both MSCs and Ang-1 played a synergistic role in reducing alveolar inflammation and permeability (11, 12). Both studies used syngeneic MSCs for cell therapy, which avoids the issue of a potential host immune response. We have overcome this limitation, showing that xenogeneic hASCs become immunomodulatory and are well tolerated when transplanted into the mouse ALI model. Indeed, in terms of safety, the increasing experience with the systemic administration of allogeneic MSCs, including a recent trial in patients with chronic obstructive pulmonary disease (45), demonstrates no obvious infusional toxicity or safety issues, although longer-term follow-up studies are needed to encourage MSC-based therapy in the clinic. Moreover, the use of hASCs as local sST2 factories in the injured lung has obvious advantages compared with alternative gene therapy strategies such as systemic, sST2-overexpressing, adenoviral vector administration (44). Because of their immunogenicity, the systemic delivery of adenovirus vectors may trigger serious adverse events (46). The transient presence of xenogeneic/allogeneic genetically engineered hASCs in the treated lungs also reduces safety concerns regarding the persistence of these implanted cells for longer than required. Furthermore, given the wide variety of cellular responses regulated by IL-33, its widespread and/or sustained inhibition through the sST2 decoy receptor should be approached with caution (47).

Finally, although our endotoxin-based mouse ALI model is very reproducible and has been used extensively (25), particularly to evaluate the potential of MSCs (9), the use of sterile injury may represent a limitation in our study. Specifically, we could infer that the blockade of IL-33 activity through the use of sST2-overexpressing hASCs might worsen outcomes in a model of bacterial pneumonia, because intravenous IL-33 supplementation has been shown to improve outcomes in a cecal ligation and puncture (CLP) model of sepsis in mice (48). Conversely, two recent reports using relevant models of bacterial pneumonia confirmed the usefulness of modulating the IL-33–ST2 axis

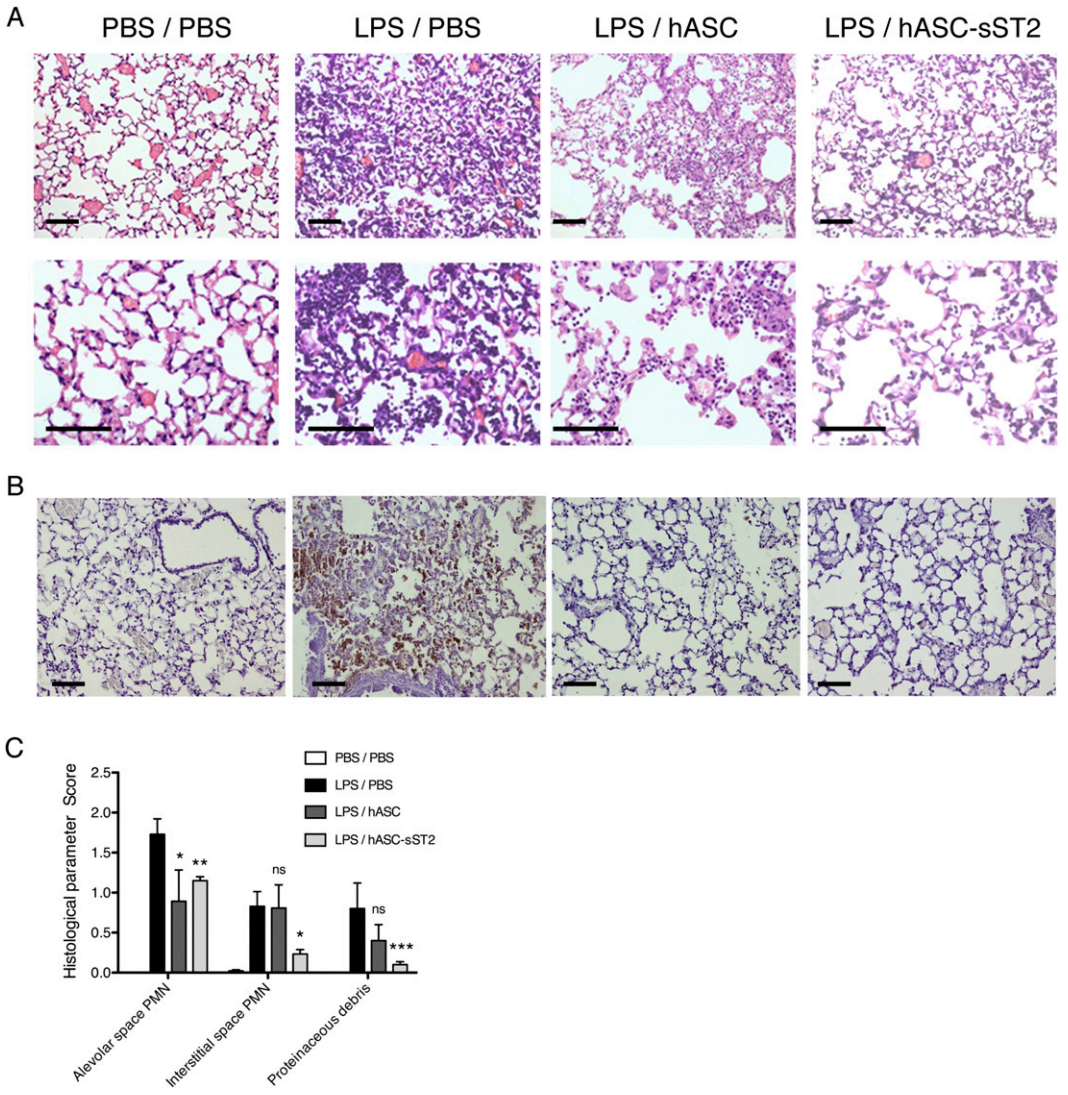

Figure 7. Lung histopathology in the mouse ALI model. Histological evaluation of the therapeutic potential of hASCs and hASC-sST2 on LPS-induced murine acute lung injury. Representative images of hematoxylin and eosin–stained (*A*) and terminal deoxynucleotidyl transferase–mediated deoxyuridine triphosphate nick-end labeling–stained (*B*) lung sections from control, PBS-instilled, untreated mice (PBS/PBS), LPS-challenged, untreated mice (LPS/PBS), LPS-challenged, hASC-treated mice (LPS/hASC), and LPS-challenged, hASC-sST2-treated mice (LPS/hASC-sST2) at low (*top* and *bottom*) and high (*middle*) magnification. *Scale bars* = 20 μm. (*C*) Histological parameter scoring included alveolar space polymorphonuclear cells (PMN), interstitial space PMN, and proteinaceous debris. PBS/PBS, PBS-instilled, untreated mice (*open columns*), LPS/PBS, LPS-challenged, untreated mice (*solid columns*); LPS/hASC, LPS-challenged, hASC-treated mice (*dark gray columns*); LPS/hASC-sST2, LPS-challenged, hASC-sST2–treated mice (*light gray columns*). Three hundred alveoli were examined per mouse. Data are presented as means ± SDs ($n = 6$–9 per group). $^{*}P < 0.05$, $^{**}P < 0.01$, and $^{***}P < 0.001$, compared with the LPS/PBS group. ns, not significant.

for lessening sepsis-induced lung injury. One approach involved ST2 knockout mice, which were protected against the lethality of secondary pneumonia with *Pseudomonas aeruginosa* during CLP-induced sepsis, possibly by inhibiting Type 1 cytokine production by T cells (49). The other approach showed that an overexpression of the ubiquitin ligase FBXL19 abrogated the proapoptotic and inflammatory effects of IL-33, and lessened the severity of lung injury in mouse models of pneumonia by an intratracheal administration of LPS or *E. coli*, selectively mediating the degradation of the ST2 receptor in the proteasome (50). Therefore, both studies supported a protective anti-inflammatory and immunomodulatory role of sST2-mediated pulmonary IL-33 blockade, stressing the importance of the model system used and/or the route of IL-33 administration, thus supporting the validity of our approach. However, additional studies, including more clinically relevant models involving sepsis and pneumonia induced by live bacteria, will be needed to reproduce our findings in the LPS-based ALI model of sterile inflammation.

In conclusion, hASCs, whether autologous or allogeneic, can be easily obtained and expanded. These cells are able to sense the immune–inflammatory environment and to reestablish the physiological epithelial/endothelial balance when retained in the injured pulmonary microvasculature, owing to their particular control over innate and adaptive immune response cells. We have supplemented the intrinsic features of hASCs by genetic engineering through local sST2 overexpression. Thus, recombinant sST2 exerts an additional protective action against the innate immune–inflammatory response occurring in ALI. Although we acknowledge the limitations of the LPS-induced lung injury model to reproduce the full complexity of clinical ALI/ARDS in human patients, our targeted gene-based and cell-based therapy was proven to restore the acute histopathological and biochemical changes occurring after endotoxin challenge of the airways. Thus, our approach may offer therapeutic potential in ALI/ARDS, although further studies using more pathophysiologically oriented ALI models will be necessary in the advance toward clinical applications.

Author disclosures are available with the text of this article at www.atsjournals.org.

Acknowledgments: The authors thank Juanjo Rojas, Sergio Martinez-Hoyer, and Andreu García for their inestimable technical help, Yolanda Fernández for her assistance with the *in vivo* imaging assay, Eva Serrano, Esther Castaño, and Eva Julià for their aid in flow cytometric assays, and Prof. Ferran Morell for his unconditional support.

References

1. Ware LB, Matthay MA. The acute respiratory distress syndrome. *N Engl J Med* 2000;342:1334–1349.
2. Acute Respiratory Distress Syndrome Network. Ventilation with lower tidal volumes as compared with traditional tidal volumes for acute

lung injury and the acute respiratory distress syndrome. *N Engl J Med* 2000;342:1301–1308.
3. National Heart, Lung, and Blood Institute Acute Respiratory Distress Syndrome Clinical Trials Network, Wiedemann HP, Wheeler AP, Bernard GR, Thompson BT, Hayden D, deBoisblanc B, Connors AF Jr, Hite RD, Harabin AL. Comparison of two fluid-management strategies in acute lung injury. *N Engl J Med* 2006;354:2564–2575.
4. Rubenfeld GD, Caldwell E, Peabody E, Weaver J, Martin DP, Neff M, Stern EJ, Hudson L-D. Incidence and outcomes of acute lung injury. *N Engl J Med* 2005;353:1685–1693.
5. Ghannam S, Bouffi C, Djouad F, Jorgensen C, Noël D. Immunosuppression by mesenchymal stem cells: mechanisms and clinical applications. *Stem Cell Res Ther* 2010;1:2.
6. English K. Mechanisms of mesenchymal stromal cell immunomodulation. *Immunol Cell Biol* 2013;91:19–26.
7. Gao J, Dennis JE, Muzic RF, Lundberg M, Caplan AI. The dynamic *in vivo* distribution of bone marrow–derived mesenchymal stem cells after infusion. *Cells Tissues Organs* 2001;169:12–20.
8. Ortiz LA, Gambelli F, McBride C, Gaupp D, Baddoo M, Kaminski N, Phinney DG. Mesenchymal stem cell engraftment in lung is enhanced in response to bleomycin exposure and ameliorates its fibrotic effects. *Proc Natl Acad Sci USA* 2003;100:8407–8411.
9. Gotts JE, Matthay MA. Mesenchymal stem cells and acute lung injury. *Crit Care Clin* 2011;27:719–733.
10. Cárdenes N, Cáceres E, Romagnoli M, Rojas M. Mesenchymal stem cells: a promising therapy for the acute respiratory distress syndrome. *Respiration* 2013;85:179–192.
11. Xu J, Qu J, Cao L, Sai Y, Chen C, He L, Yu L. Mesenchymal stem cell–based angiopoietin-1 gene therapy for acute lung injury induced by lipopolysaccharide in mice. *J Pathol* 2008;214:472–481.
12. Mei SH, McCarter SD, Deng Y, Parker CH, Liles WC, Stewart DJ. Prevention of LPS-induced acute lung injury in mice by mesenchymal stem cells overexpressing angiopoietin 1. *PLoS Med* 2007;4:e269.
13. Yagami A, Orihara K, Morita H, Futamura K, Hashimoto N, Matsumoto K, Saito H, Matsuda A. IL-33 mediates inflammatory responses in human lung tissue cells. *J Immunol* 2010;185:5743–5750.
14. Palmer G, Gabay C. Interleukin-33 biology with potential insights into human diseases. *Nat Rev Rheumatol* 2011;7:321–329.
15. Sweet MJ, Leung BP, Kang D, Sogaard M, Schulz K, Trajkovic V, Campbell CC, Xu D, Liew FY. A novel pathway regulating lipopolysaccharide-induced shock by ST2/T1 via inhibition of Toll-like receptor 4 expression. *J Immunol* 2001;166:6633–6639.
16. Moreno R, Martínez I, Petriz J, Nadal M, Tintoré X, Gonzalez JR, Gratacós E, Aran JM. The β-interferon scaffold attachment region confers high-level transgene expression and avoids extinction by epigenetic modifications of integrated provirus in adipose tissue–derived human mesenchymal stem cells. *Tissue Eng Part C Methods* 2011;17:275–287.
17. Doherty M, Todd D, McFerran N, Hoey EM. Sequence analysis of a porcine enterovirus serotype 1 isolate: relationships with other picornaviruses. *J Gen Virol* 1999;80:1929–1941.
18. Moreno R, Martínez-González I, Rosal M, Nadal M, Petriz J, Gratacós E, Aran JM. Fetal liver–derived mesenchymal stem cell engraftment after allogeneic *in utero* transplantation into rabbits. *Stem Cells Dev* 2012;21:284–295.
19. Ibrahimi A, Vande Velde G, Reumers V, Toelen J, Thiry I, Vandeputte C, Vets S, Deroose C, Bormans G, Baekelandt V, *et al*. Highly efficient multicistronic lentiviral vectors with peptide 2A sequences. *Hum Gene Ther* 2009;20:845–860.
20. Liu H, Liu S, Li Y, Wang X, Xue W, Ge G, Luo X. The role of SDF-1–CXCR4/CXCR7 axis in the therapeutic effects of hypoxia-preconditioned mesenchymal stem cells for renal ischemia/reperfusion injury. *PLoS ONE* 2012;7:e34608.
21. Prockop DJ, Oh JY. Mesenchymal stem/stromal cells (MSCs): role as guardians of inflammation. *Mol Ther* 2012;20:14–20.
22. Moulin D, Donzé O, Talabot-Ayer D, Mézin F, Palmer G, Gabay C. Interleukin (IL)–33 induces the release of pro-inflammatory mediators by mast cells. *Cytokine* 2007;40:216–225.
23. Chignard M, Balloy V. Neutrophil recruitment and increased permeability during acute lung injury induced by lipopolysaccharide. *Am J Physiol Lung Cell Mol Physiol* 2000;279:L1083–L1090.
24. Yin H, Li X, Yuan B, Zhang B, Hu S, Gu H, Jin X, Zhu J. Heme oxygenase–1 ameliorates LPS-induced acute lung injury correlated with downregulation of interleukin-33. *Int Immunopharmacol* 2011;11:2112–2117.
25. Matute-Bello G, Downey G, Moore BB, Groshong SD, Matthay MA, Slutsky AS, Kuebler WM, Acute Lung Injury in Animals Study Group. An official American Thoracic Society workshop report: features and measurements of experimental acute lung injury in animals. *Am J Respir Cell Mol Biol* 2011;44:725–738.
26. Rochefort GY, Vaudin P, Bonnet N, Pages JC, Domenech J, Charbord P, Eder V. Influence of hypoxia on the domiciliation of mesenchymal stem cells after infusion into rats: possibilities of targeting pulmonary artery remodeling via cells therapies? *Respir Res* 2005;6:125.
27. Schrepfer S, Deuse T, Reichenspurner H, Fischbein MP, Robbins RC, Pelletier MP. Stem cell transplantation: the lung barrier. *Transplant Proc* 2007;39:573–576.
28. Németh K, Keane-Myers A, Brown JM, Metcalfe DD, Gorham JD, Bundoc VG, Hodges MG, Jelinek I, Madala S, Karpati S, *et al*. Bone marrow stromal cells use TGF-beta to suppress allergic responses in a mouse model of ragweed-induced asthma. *Proc Natl Acad Sci USA* 2010;107:5652–5657.
29. Vilalta M, Dégano IR, Bagó J, Gould D, Santos M, García-Arranz M, Ayats R, Fuster C, Chernajovsky Y, García-Olmo D, *et al*. Biodistribution, long-term survival, and safety of human adipose tissue–derived mesenchymal stem cells transplanted in nude mice by high sensitivity non-invasive bioluminescence imaging. *Stem Cells Dev* 2008;17:993–1004.
30. Maggini J, Mirkin G, Bognanni I, Holmberg J, Piazzón IM, Nepomnaschy I, Costa H, Cañones C, Raiden S, Vermeulen M, *et al*. Mouse bone marrow–derived mesenchymal stromal cells turn activated macrophages into a regulatory-like profile. *PLoS ONE* 2010;5:e9252.
31. Delarosa O, Sánchez-Correa B, Morgado S, Ramírez C, del Río B, Menta R, Lombardo E, Tarazona R, Casado JG. Human adipose–derived stem cells impair natural killer cell function and exhibit low susceptibility to natural killer–mediated lysis. *Stem Cells Dev* 2012;21:1333–1343.
32. Sun J, Han Z-B, Liao W, Yang SG, Yang ZX, Yu JX, Meng L, Wu R, Han ZC. Intrapulmonary delivery of human umbilical cord mesenchymal stem cells attenuates acute lung injury by expanding $CD4^+CD25^+$ Forkhead Boxp3 $(Foxp3)^+$ regulatory T cells and balancing anti- and pro-inflammatory factors. *Cell Physiol Biochem* 2011;27:587–596.
33. Kim ES, Chang YS, Choi SJ, Kim JK, Yoo HS, Ahn SY, Sung DK, Kim SY, Park YR, Park WS. Intratracheal transplantation of human umbilical cord blood–derived mesenchymal stem cells attenuates *Escherichia coli*–induced acute lung injury in mice. *Respir Res* 2011;12:108.
34. Li J, Li D, Liu X, Tang S, Wei F. Human umbilical cord mesenchymal stem cells reduce systemic inflammation and attenuate LPS-induced acute lung injury in rats. *J Inflamm* 2012;9:33.
35. Zhang S, Danchuk SD, Imhof KMP, Semon JA, Scruggs BA, Bonvillain RW, Strong AL, Gimble JM, Betancourt AM, Sullivan DE, *et al*. Comparison of the therapeutic effects of human and mouse adipose-derived stem cells in a murine model of lipopolysaccharide-induced acute lung injury. *Stem Cell Res Ther* 2013;4:13.
36. Danchuk S, Ylostalo JH, Hossain F, Sorge R, Ramsey A, Bonvillain RW, Lasky JA, Bunnell BA, Welsh DA, Prockop DJ, *et al*. Human multipotent stromal cells attenuate lipopolysaccharide-induced acute lung injury in mice via secretion of tumor necrosis factor–α–induced protein 6. *Stem Cell Res Ther* 2011;2:27.
37. Lee JW, Fang X, Gupta N, Serikov V, Matthay MA. Allogeneic human mesenchymal stem cells for treatment of *E. coli* endotoxin–induced acute lung injury in the *ex vivo* perfused human lung. *Proc Natl Acad Sci USA* 2009;106:16357–16362.
38. Lee JW, Krasnodembskaya A, McKenna DH, Song Y, Abbot J, Matthay MA. Therapeutic effects of human mesenchymal stem cells in *ex vivo* human lungs injured with live bacteria. *Am J Respir Crit Care Med* 2013;187:751–760.
39. Oboki K, Ohno T, Kajiwara N, Saito H, Nakae S. IL-33 and IL-33 receptors in host defense and diseases. *Allergol Int* 2010;59:143–160.
40. Pichery M, Mirey E, Mercier P, Lefrancais E, Dujardin A, Ortega N, Girard P. Endogenous IL-33 is highly expressed in mouse epithelial barrier tissues, lymphoid organs, brain, embryos, and inflamed tissues: *in situ* analysis using a novel Il-33–lacZ gene trap reporter strain. *J Immunol* 2012;188:3488–3495.
41. Oboki K, Ohno T, Kajiwara N, Arae K, Morita H, Ishii A, Nambu A, Abe T, Kiyonari H, Matsumoto K, *et al*. IL-33 is a crucial amplifier of

innate rather than acquired immunity. *Proc Natl Acad Sci USA* 2010; 107:18581–18586.

42. Kitamura Y, Hashimoto S, Mizuta N, Kobayashi A, Kooguchi K, Fujiwara I, Nakajima H. Fas/FasL-dependent apoptosis of alveolar cells after lipopolysaccharide-induced lung injury in mice. *Am J Respir Crit Care Med* 2001;163:762–769.
43. Vanoirbeek JA, Rinaldi M, De Vooght V, Haenen S, Bobic S, Gayan-Ramirez G, Hoet PH, Verbeken E, Decramer M, Nemery B, *et al.* Noninvasive and invasive pulmonary function in mouse models of obstructive and restrictive respiratory diseases. *Am J Respir Cell Mol Biol* 2010;42:96–104.
44. Yin H, Li XY, Yuan BH, Zhang BB, Hu SL, Gu HB, Jin XB, Zhu JY. Adenovirus-mediated overexpression of soluble ST2 provides a protective effect on lipopolysaccharide-induced acute lung injury in mice. *Clin Exp Immunol* 2011;164:248–255.
45. Weiss DJ, Casaburi R, Flannery R, Leroux-Williams M, Tashkin DP. A placebo-controlled randomized trial of mesenchymal stem cells in chronic obstructive pulmonary disease. *Chest* 2013;143:1590–1598.
46. Marshall E. Gene therapy death prompts review of adenovirus vector. *Science* 1999;286:2244–2245.
47. Mato N, Fujii M, Hakamata Y, Kobayashi E, Sato A, Hayakawa M, Ohto-Ozaki H, Bando M, Ohno S, Tominaga S, *et al.* Interleukin-1 receptor–related protein ST2 suppresses the initial stage of bleomycin-induced lung injury. *Eur Respir J* 2009;33:1415–1428.
48. Alves-Filho JC, Sônego F, Souto FO, Freitas A, Verri WA Jr, Auxiliadora-Martins M, Basile-Filho A, McKenzie AN, Xu D, Cunha FQ, *et al.* Interleukin-33 attenuates sepsis by enhancing neutrophil influx to the site of infection. *Nat Med* 2010;16:708–712.
49. Hoogerwerf JJ, Leendertse M, Wieland CW, de Vos AF, de Boer JD, Florquin S, van der Poll T. Loss of suppression of tumorigenicity 2 (ST2) gene reverses sepsis-induced inhibition of lung host defense in mice. *Am J Respir Crit Care Med* 2011;183:932–940.
50. Zhao J, Wei J, Mialki RK, Mallampalli DF, Chen BB, Coon T, Zou C, Mallampalli RK, Zhao Y. F-box protein FBXL19-mediated ubiquitination and degradation of the receptor for IL-33 limits pulmonary inflammation. *Nat Immunol* 2012;13:651–658.